SPATIAL-TEMPORAL-FREQUENCY DECOMPOSITION FOR 3D MIMO MICROCELLULAR ENVIRONMENTS

Hamidreza Saligheh Rad, Saeed Gazor

Department of Electrical and Computer Engineering
Queen's University, Kingston, Ontario, K7L 3N6
radh@ee.queensu.ca

Kamal Shahtalebi

Department of Electrical Engineering,
Shahrekord University, Shahrekord, Iran
shahtalebi@wongfaye.com

***Abstract*—*A three-dimensional (3D) model is proposed for Multiple-Input Multiple-Output (MIMO) microcell Rayleigh fading channels with an ample number of scatterers. We assume appropriate probability density functions (pdfs) for relevant physical parameters of the complex scattering media. The impact of these parameters are discussed using the expression of the Correlation Function (CF) between each of the two sub-channels of the MIMO channel. The CF is decomposable into several components that describe spatial, temporal, and frequency characteristics of the MIMO communication system. Such a decomposition allows easier investigation and gives a better understanding of the full potential of MIMO wireless communications. The describing components do not always have closed-form expressions. Therefore, closed-form expressions are obtained for some special cases. In practice, a linear convex combination of the expressions from these cases can approximate almost any model of microcellular environments. The proposed model is a generalization of several existing models including the Jake's/Clark model.*

I. INTRODUCTION

The three-dimensional (3D) Multiple-Input Multiple-Output (MIMO) channel modeling has attracted the attention of several researchers, e.g., [1]–[6]. Each of these researchers have contributed to this process by introducing more relevant physical parameters describing the propagation environment. The expression of the Correlation Function (CF) requires numerical evaluation for most existing 3D-MIMO models. Some interesting closed-form expressions for the CF are proposed in [7] for a 2D environment and narrowband signals. In a 3D environment they have also considered the uniform distribution of scatterers on the elevation angle. With the exception of the authors of [8], who have noticed that the CF matrix for a 2D MIMO propagation environment can be decomposed under certain reasonable assumptions, this issue has been virtually ignored.

In this paper, we consider the CF of the 3D MIMO microcellular wireless environments and decompose the CF into spatial, temporal and frequency components based on 2D and 3D models proposed in [9], [10]. Such a decomposition gives better insight into understanding the potential of MIMO systems. Using such a decomposition, the generation of simulated MIMO channels becomes easier. The considered 3D model takes into account the behavior of the channel with respect to: the MS motion; Elevation Angle (EA) spread and azimuthal angle spread; arbitrary antenna array geometry; random phase change in the received waveform; and, the carrier frequencies. The geometry of scatterers is modeled in a flexible way by the pdfs of the physical parameters and can fit easily into different environments. In other words, this model describes statistical characteristics of the 3D Rayleigh MIMO-channel as a function of space, time, and frequency.

CCECE 2004- CCGEI 2004, Niagara Falls, May/mai 2004 0-7803-8253-6/04/$17.00 2004 IEEE

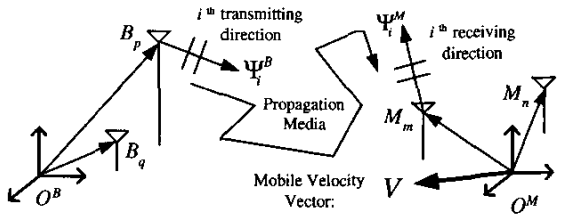

Fig. 1. p^{th} antenna of the BS and m^{th} antenna of the MS in their local coordinate axis in a 3D wave propagation environment. The time-delay of the i^{th} propagating waveform has three different components: two small relative propagation delays and one major distance delay.

The remainder of this paper is organized as follows: Section II presents the notations and assumptions of a 3D MIMO channel model. Section III describes the propagation environment and calculates the CF for the 3D Rayleigh fading channel in some important cases. Section IV decomposes the expression of the CF of the 3D model into some positive functions. Section V summarizes The pros and cons of this modeling method.

II. 3D MIMO CHANNEL

Figure 1 shows a pair of BS-MS antenna elements from a multielement antenna system in a 3D wave propagation environment. Similar to [9] and [10], the following notations are used where the superscripts B and M indicate variables at the BS and the MS sides respectively, while subscript i indicates the variable related to the i^{th} dominant path:

- O^B BS coordinate and O^M is MS coordinate;
- ω Carrier frequency;
- V MS speed vector;

c Wave propagation velocity;
B_p Position of the p^{th} antenna element on the BS side relative to O^B;
M_m Position of the m^{th} antenna element on the MS side relative to O^M;
Ψ_i^B The unity vector pointing to the Direction of Departure (DOD) from the BS;
Ψ_i^M The unity vector pointing to the Direction of Arrival (DOA);
Θ_i^B The DOD azimuthal angle from the BS;
Θ_i^M The DOA azimuthal angle to the MS;
Ω_i^B The DOD elevation angle from the BS;
Ω_i^M The DOA elevation angle to the MS;
I Number of total dominant paths;
$\tau_{p,m;i}$ Time delay between p^{th} BS and m^{th} MS antenna elements;
$g_{p,m;i}$ Gain between p^{th} BS antenna element and m^{th} MS antenna element, approximated by g_i;
ϕ_i Phase change;
ϖ_i The shifted frequency by the Doppler effect;
β_i Fast fading factor;
η Pathloss exponent;
θ The parameter describing the uniform distribution for the phase change;
α Degree of urbanization in the pdf of EA;
σ Variance of the time-delay profile;
$\overline{\tau}$ Mean of the time-delay profile.

Note $\Psi_i \triangleq [\cos(\Omega_i)\cos(\Theta_i), \cos(\Omega_i)\sin(\Theta_i), \sin(\Omega_i)]^T$ [14].

A solution basis for Maxwell's equation is to break down the received waveform into a linear combination of a set of planar waves [11], [13]. Planar waves emitted from the array element B_p are scattered in the propagation media and travel over several dominant paths with different lengths. The Channel Impulse Response (CIR) expressing the scenario is written as

$$h_{mp}(t,\omega) = \frac{1}{\sqrt{I}} \sum_{i=1}^{I} g_{p,m;i} e^{j\phi_i + j\varpi_i t - j\omega\tau_{p,m;i}}, \quad (1)$$

where the real gain $g_{p,m;i}/\sqrt{I}$ is a function of the time-delay and the fast fading factor [12]. The frequency of the i^{th} received waveform is denoted by $\varpi_i \triangleq \omega(1 + \frac{V^T \Psi_i^M}{c})$, where ω is the carrier frequency and $(1 + \frac{V^T \Psi_i^M}{c})$ is the Doppler spread factor.

III. STATISTICAL MICROCEL MODEL

The model used in this paper is based on some assumptions about the physical parameters which are explained here (for more details [9]–[13]):

A1) We decompose i^{th} path propagation delay, $\tau_{p,m;i}$, as:

$$\tau_{p,m;i} = \tau_i - (\tau_{p;i}^B + \tau_{m;i}^M), \quad (2a)$$

$$\tau_{p;i}^B \triangleq \frac{B_p^T \Psi_i^B}{c}, \quad (2b)$$

$$\tau_{m;i}^M \triangleq \frac{M_m^T \Psi_i^M}{c}, \quad (2c)$$

where τ_i represents delay between O^B and O^M, and $\tau_{p;i}^B$ and $\tau_{m;i}^M$ represent relative delays from antenna elements, B_p or M_m. We assume that τ_i are independent identically distributed (i.i.d.) with pdf $\tau_i \sim \frac{1}{\sigma} e^{-\frac{\tau - \overline{\tau} + \sigma}{\sigma}}$, $\forall \tau \geqslant \overline{\tau} - \sigma$, where $\overline{\tau}$ is the average time-delay related to the propagation distance and σ is the variance of delay. Moment Generating Function (MGF) of τ_i is $\Phi_\tau(s) = \frac{e^{(\overline{\tau}-\sigma)s}}{1-\sigma s}$.

A2) Path gain, $g_{p,m;i}$, and propagation delay, $\tau_{p,m;i}$, are dependent as follows [12], [13]:

$$g_{p,m;i} \triangleq \beta_i \sqrt{P(\tau_{p,m;i})} = \beta_i \sqrt{\left(\frac{\tau_{p,m;i}}{\overline{\tau}}\right)^{\eta} P_o}, \quad (3)$$

where $P(\tau_{p,m;i})$ is the average pathloss power, β_i is the fast fading factor, η is called pathloss exponent, and P_o is a constant [12], [13]. The β_i is assumed to be stationary, and independent of the time-delay, $\tau_{p,m;i}$. Depending on the characteristics of the media, the pathloss exponent is usually measured between 2 and 6 [12]. From (3), (2a) and the obvious fact that $|\tau_i| \gg \max\{|\tau_{p;i}^B|, |\tau_{m;i}^M|\}$, we approximate $P(\tau_{p,m;i}) \simeq P(\tau_i)$ $\forall p, m$ as:

$$g_{p,m;i} \simeq g_i = \beta_i \left(\frac{\tau_i}{\overline{\tau}}\right)^{\frac{\eta}{2}} \sqrt{P_o}. \quad (4)$$

A3) The phase contribution of scatterers are considered by a random phase change, ϕ_i, as: $p_{\boldsymbol{\phi}}(\phi) \sim U[0, 2\theta)$; $0 \leqslant \theta < \pi$, and θ is the softness factor. The random phase change, ϕ_i, is independent from channel gain, time-delay, and fast fading factor, β_i.

A4) The azimuthal angles are all uniformly distribution over $(-\pi, \pi]$, i.e, Θ_i^B and $\Theta_i^M \sim U(-\pi, \pi]$. This assumption characterizes a microcell propagation environments.

A5) Determination of i.i.d. pdf of elevation angles requires some considerations of environment parameters, e.g., as degree of urbanization [2]. We consider a family of distributions for $|\Omega| \leqslant \frac{\pi}{2}$ as [7]:

$$p_{\boldsymbol{\Omega}}(\Omega) = \frac{\Gamma(\alpha+1)\cos^{2\alpha}(\Omega)}{\sqrt{\pi}\,\Gamma(\alpha+\frac{1}{2})}, \quad (5)$$

where $\Gamma(z) = \int_0^\infty \xi^{z-1} e^{-\xi} d\xi$ is the Gamma function [14, Page 258], and $\alpha \geqslant 0$ is related to the degree of urbanization. This parameter specifies the type of the environment related to the amount of wave scattered into the third dimension of the space. Moreover, a linear convex mixture from this class as a pdf covers a wide class of distributions and can realistically model a microcellular environment. Therefore, a linear convex mixture of obtained results characterizes a wide class of environments. Experimental data can be used to interpolate for the calculation of this linear combination.

We derive a closed-from expression for the CF between CIRs of two arbitrary communication links, $h_{mp}(t_1, \omega_1)$ and $h_{nq}(t_2, \omega_2)$, denoted by

$$R_{mp,nq}(t_1, t_2; \omega_1, \omega_2) \triangleq E[h_{mp}(t_1, \omega_1) h_{nq}^*(t_2, \omega_2)]. \quad (6)$$

Replacing (1), (2), and (4) in (6), considering the characteristics of a planar wave [10], [11], using assumptions A1-A5 established in this section, and doing some manipulations, $R_{mp,nq}(t_1,t_2;\omega_1,\omega_2)$ is decomposed as follows:

$$\frac{1}{I}\sum_{i_1=1}^{I}\sum_{i_2=1}^{I} E\left[g_{i_1}g_{i_2}\exp\left(j\left(\omega_2\tau_{i_2}-\omega_1\tau_{i_1}\right)\right)\right] \times E\left[\exp(j(\phi_{i_1}-\phi_{i_2}))\right]\times E_{\Omega^B}\times E_{\Omega^M}, \quad (7)$$

where,

$$\begin{aligned} E_{\Omega^B} &\triangleq E\left[e^{\Lambda_1^B\sin(\Omega^B)}J_0\left(\Lambda_2^B\cos(\Omega^B)\right)\right],\\ E_{\Omega^M} &\triangleq E\left[e^{\Lambda_1^M\sin(\Omega^M)}J_0\left(\Lambda_2^M\cos(\Omega^M)\right)\right],\\ d^B &\triangleq \omega_1 B_p-\omega_2 B_q,\\ d^M &\triangleq (\omega_1 t_1-\omega_2 t_2)V+(\omega_1 M_m-\omega_2 M_n),\\ \Lambda_1 &\triangleq d_z/c \text{ and } \Lambda_2\triangleq\sqrt{(d_x)^2+(d_y)^2}/c, \end{aligned}$$

$d=[d_x,\ d_y,\ d_z]^T$, and $J_0(z)\triangleq\frac{1}{2\pi}\int_0^{2\pi}e^{jz\cos\xi}d\xi$.

The terms E_{Ω^B} and E_{Ω^M} do not always have a closed-form expression; therefore, we give closed-form solutions for suggested basis pdfs in (5). The expressions of E_{Ω^B} and E_{Ω^M} are similar; for this reason, we we drop the superscripts $(.)^B$ or $(.)^M$ and use E_Ω for both E_{Ω^B} and E_{Ω^M}. Thus, the microcellular wireless wave propagation media is modeled under a large variety of different situations that may happen in reality.

Case $d_x=d_y=0$: This case studies the vertical separation of antenna elements located at the origin of azimuthal plane in a microcellular propagation environment. Using the Bessel integration [14, Page 360], we get

$$E_\Omega=\frac{\Gamma(\alpha+1)}{(\frac{1}{2}\Lambda_1)^\alpha}\,J_\alpha(\Lambda_1). \quad (8)$$

Different values of α represents different environments.

Case $\alpha=0$, $d_z=0$: A uniform 3D rich scattering environment. Using Bessel integration [14, Page 485], we get

$$E_\Omega=J_0^2\left(\|d\|/(2c)\right). \quad (9)$$

This result is similar to the 2D scenario; however, this model is a direct 3D extension of the Jake's/Clarke model for a microcellular rich scattering environment [10].

Case $\alpha=\frac{1}{2}$, $d_z=0$: Scatterers are uniformly distributed on sphere. Using Bessel integration [14, Page 485], we get

$$E_\Omega=\sqrt{\frac{\pi}{2\Lambda_2}}\,J_{\frac{1}{2}}(\Lambda_2). \quad (10)$$

Considering the point $J_{\frac{1}{2}}(z)=\sqrt{\frac{2}{\pi}}\frac{\sin(z)}{\sqrt{z}}$ [14, Page 437], the result will be in the form of a sinusoid as

$$E_\Omega=\frac{\sin(\Lambda_2)}{\Lambda_2}\triangleq\operatorname{sinc}(\Lambda_2). \quad (11)$$

This result is consistent with literature [7].

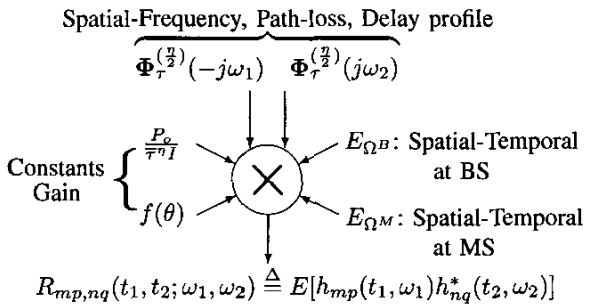

Fig. 2. Decomposition of the CF of a 3D-MIMO Microcellular Wireless Channel. Each group talks about some special features in the propagation environment.

Considering expectations in (7) and replacing (4) in that equation, using Assumption 3, MGF of the time-delay, MGF of i.i.d. phase changes[1], we get

$$R_{mp,nq}(t_1,t_2;\omega_1,\omega_2)=\frac{P_o}{\overline{\tau}^\eta I}\times\left(\sum_{i=1}^{I}E[\beta_i^2]+\left(\frac{\sin\theta}{\theta}\right)^2\sum_{\substack{i_1,i_2=1\\ i_1\neq i_2}}^{I}E[\beta_{i_1}\beta_{i_2}]\right) \times E_{\Omega^B}E_{\Omega^M}\Phi_\tau^{(\frac{\eta}{2})}(-j\omega_1)\Phi_\tau^{(\frac{\eta}{2})}(j\omega_2), \quad (13)$$

where E_Ω^B and E_Ω^M are calculated in some special cases in this section, and $\Phi_\tau^{(\frac{\eta}{2})}(s)$ is obtained by $(\frac{\eta}{2})^{\text{th}}$-times differentiating the MGF, $\Phi_\tau(s)$ [14]. We assume that $\frac{\eta}{2}$ is a positive integer number [2]. The closed-form calculation of these two expectation considering the time-delay distribution in Assumption A1 is proposed in [9] as: $e^{j(\overline{\tau}-\sigma)(\omega_2-\omega_1)}\sum_{l_1,l_2=0}^{\frac{\eta}{2}}\frac{(\frac{\eta}{2})!^2\,\sigma^{l_1+l_2}(\overline{\tau}-\sigma)^{\eta-(l_1+l_2)}}{(\frac{\eta}{2}-l_1)!(\frac{\eta}{2}-l_2)!(1+j\sigma\omega_1)^{l_1+1}(1-j\sigma\omega_2)^{l_2+1}}$. The effect of slow fading is taken into account in the log-normal component by Assumption A2 [13], while β_i is assumed to be time-invariant [12], [13]. One should note that only the second line in (13), $f(\theta)$, depends on the fast fading gains β_i and softness factor θ.

IV. DECOMPOSITION OF CF

In this paper, our analysis of a 3D-MIMO mirocellular environment is based on the decomposability of the CF into disjoint components describing spatial, temporal, and frequency characteristics of the MIMO system. Figure 2 shows this decomposition of the CF. Such a decomposition allows easier investigation and gives a better understanding

[1] Using Assumption A3, we have

$$E\left[e^{j(\phi_{i_1}-\phi_{i_2})}\right]=\begin{cases}1 & i_1=i_2,\\ \Phi_{\phi_{i_1}}(j)\Phi_{\phi_{i_2}}(-j) & i_1\neq i_2,\end{cases} \quad (12)$$

where $\Phi_{\phi_i}(s)=\frac{e^{s\theta}-e^{-s\theta}}{2s\theta}$ is the MGF of ϕ_i.

[2] The appropriate values for the pathloss is $\eta=2$ for free propagation environments, $\eta=4$ for rural environments, and $\eta=6$ for crowded urban environments [12], [13].

of the full potential of MIMO wireless communications. Each of these components has an exact and unique role in order to express the effects of MS, BS, or the complicated propagation environment on the CF. Therefore, we are able to analyze the 3D-MIMO microcellular wireless channel easily by looking at these components: E_{Ω^B}, E_{Ω^M}, $\frac{P_o}{\overline{\tau}^{\eta}I}$, $f(\theta)$, $\mathbf{\Phi}_{\tau}^{(\frac{\eta}{2})}(-j\omega_1)$ and $\mathbf{\Phi}_{\tau}^{(\frac{\eta}{2})}(j\omega_2)$. Based on the role of each component, they are classified in three different categories as follows:

- E_{Ω^B} and E_{Ω^M} talk about the spatial-frequency aspects of the 3D-MIMO propagation environment at the BS or MS, respectively. These two items contain the influence of spatial angles for the DOA (azimuth and elevation angles) affecting the CF; geometry of antenna arrays at the BS or MS; the effect of the carrier frequency used in each antenna element; the effect of mobile speed at the MS; and, the effect of time indices used to sample the CF. Interestingly, the Doppler effect caused by the mobile speed is combined with the effect of the location of antenna elements and the time index. For instance, in a fixed carrier frequency, $\omega_1 = \omega_2$, the proposed function depends on the time difference, $t_1 - t_2$ (i.e., the model offers a stationary process in a narrowband system). One should note that if both antenna elements use the same carrier frequency, their relative distance will affect the modeling function. This property is important when the 3D model investigates the effect of vertical separation of antenna elements because of their different heights.
- $\mathbf{\Phi}_{\tau}^{(\frac{\eta}{2})}(-j\omega_1)$ and $\mathbf{\Phi}_{\tau}^{(\frac{\eta}{2})}(j\omega_2)$ mainly discuss about the frequency aspects of the 3D-MIMO propagation environment. The dependency of the CF on the carrier frequencies, ω_1, ω_2 via these components shows that the correlation decreases when these frequencies or their differences, increase. This result is also consistent with the literature. The effect of the type of the environment η is reflected on the times we differentiate the MGF of the time-delay. This is addressed as an important feature this model.
- The last two components, $f(\theta)$ and $\frac{P_o}{\overline{\tau}^{\eta}I}$, investigate the spatial-frequency aspects of the 3D-MIMO propagation environment as well as the effect of different physical parameters of the complex propagation media between BS and MS. The second line in (13) is a constant gain and also represents the effect of fast fading factors, β_i and softness factor, θ. As all $\{\beta_i\}_{i=1}^{I}$ are positive, this term takes its maximum at $\theta = 0$; therefore, an environment with no phase contribution on the received waveform produces the largest gain. This is expected because an environment with random phase introduces more randomness in channel [11]. This constant gain, which plays an important role in the communication performance, is determined by the following limited statistics: $\theta, \sum_i E[\beta_i^2]$, and $E[|\sum_i \beta_i|^2]$. Fast fading factors, β_i, are often assumed to be Rayleigh distributed, and can be approximated by some simplifying assumptions based on the physical characteristics of the propagation media [12]. The spatial effects of the propagation media comes into parameters of the distribution assigned to describe the time delay, $\overline{\tau}$ and σ. These two parameters depend on the type of the environment, which is characterized by η, and the distance between BS and MS. Another point in this component is the role of η, which distinguishes between several environments of wave propagation.

V. CONCLUSIONS

The expression of the CF of 3D-MIMO microcellular Rayleigh fading channels is decomposed into a number of components (i.e., E_{Ω^B}, E_{Ω^B}, $\mathbf{\Phi}_{\tau}^{(\frac{\eta}{2})}(-j\omega_1)\mathbf{\Phi}_{\tau}^{(\frac{\eta}{2})}(j\omega_2)$), a constant term and another term describing the impact of the softness factor and the channel gains. All these terms are non-negative definite CFs. The terms E_{Ω^B} and E_{Ω^B} describe the spatial-temporal effects of the BS and MS, respectively. Other terms describe spatial-frequency aspects of propagation media. Such a decomposition allows easier investigation and gives better understanding of the full potential of MIMO wireless communications. [8].

REFERENCES

[1] T. Aulin, "A Modified Model for the Fading Signal at a Mobile Radio Channel," *IEEE Transactions on Vehicular Technology,* vol. VT-28, no. 3, pp. 182-203, August 1979.

[2] J. D. Parson, and A. M. D. Turkmani, "Characterisation of Mobile Radio Signals: Model Description," *IEE Proceedings I, Communications, Speech and Vision,* vol. 138, no. 6, pp. 549-556, December 1991.

[3] ——, "Characterisation of Mobile Radio Signals: Base Station Crosscorrelation," *IEE Proceedings I, Communications, Speech and Vision,* vol. 138, pp. 557-565, December 1991.

[4] R. H. Clarke, W. L. Khoo, "3-D mobile radio channel statistics," *IEEE Transactions on Vehicular Technology,* vol. 46, no. 3, pp. 798-799, August 1997.

[5] S. Roy, and D. D. Falconer, "A Three-Dimensional Wideband Propagation Model for the Study of Base Station Antenna Arrays with Application to LMCS," *Presented at VTC'98,* Ottawa, August 1998.

[6] Y. Z. Mohasseb, and M. P. Fitz, "A 3D Spatio-Temporal Simulation Model for Wireless Channels," *IEEE Journal on Selected Areas in Communications,* vol. 20, no. 6, August 2002.

[7] P. D. Teal, T. D. Abhayapala, and R. A. Kennedy, "Spatial correlation for general distributions of scatterers," *IEEE Signal Processing Letters,* vol. 9, no. 10, pp. 305-308, October 2002.

[8] T. D. Abhayapala, T. S. Pollock, and R. A. Kennedy, "Spatial Decomposition of MIMO Wireless Channels," *International Symposium on Signal Processing and its Applications 2003 (ISSPA'03),* Paris, France, 2003.

[9] H. S. Rad, S. Gazor, K. Shahtalebi, "A 3D Wireless Channel Model for MIMO Microcell Environments," submitted to *12th Iranian Conference on Electrical Engineering (ICEE'04),* November 2003.

[10] S. Gazor, and H. S. Rad, "Multi-Transmitter Multi-Receiver Wireless Channel Model for Isotropic Scattering Environments," submitted to *IEEE Trans. on Wireless Communications,* October 2003.

[11] G. Durgin, *Space-Time Wireless Channels*, NJ: Prentice Hall, 2003.

[12] H. L. Bertoni, *Radio Propagation for Modern Wireless Systems*, Prentice Hall PTR, 1999.

[13] S. Saunders, *Antennas and Propagation for Wireless Communication Systems*, New York: Wiley, 1999.

[14] M. Abramowitz, and I. A. Stegun, *Handbook of Mathematical Functions with Formulas, Graphs, and Mathematical Table,* Dover Publications INC., NY, June 1974.